

# Collision rates in near-resonant optical lattices

Jyrki Piilo

*Helsinki Institute of Physics, PL 64, FIN-00014 Helsingin yliopisto, Finland*

We present a simple method to calculate the binary collision rate between atoms in near-resonant optical lattices. The method is based on the Monte Carlo wave function simulations and the collision rate is obtained by monitoring the quantum flux beyond the average distance between the atoms. To illustrate the usefulness of the method, we calculate the collision rates for a wide range of occupation densities and various modulation depths of the lattice. The method presented here combined with the semiclassical calculations accounting for intra-well collisions can simplify the study of the effects of binary collisions on the dynamics of atomic clouds trapped in near-resonant optical lattices.

© 2018 Optical Society of America  
OCIS codes: 020.2070, 020.7010

## 1. Introduction

A periodic polarization or intensity gradient of a laser field can create a periodic optical potential structure for atoms. When atoms move in this structure, they may undergo Sisyphus cooling, and finally localize into the optical lattice sites<sup>1,2,3,4,5,6,7</sup>. After localization, atoms are still able to move around in the lattice. The optical-pumping-induced motion typically dominates in near-resonant optical lattices, whereas in shallow far-off resonant lattices the quantum mechanical tunneling of atoms between the lattice sites may dominate the atomic motion. Because of their ability to move between the lattice sites, two atoms may end up in the same site and collide. The purpose of this paper is to present a simple method to calculate the binary collision rate in a near-resonant optical lattice.

Cold collisions have been widely studied in magneto-optical traps<sup>8,9</sup>. This is not the case for optical lattices where the complications arise due to the position dependent coupling between the multi-level atoms and the laser field. So far, to the best of our knowledge, there has been only a few experimental cold collision studies in optical lattices<sup>10,11</sup>. Theoretical studies of the interactions between atoms in optical lattices include the mean-field type approaches<sup>12,13,14,15,16</sup>, and Monte Carlo wave function (MCWF) simulations of binary collisions in red detuned<sup>17,18</sup> and blue detuned lattices<sup>19</sup>. However, the mean-field approaches neglect the dynamical nature of the collisions, and the MCWF simulations for two atoms colliding in optical lattice require extremely large computer resources<sup>18</sup>. It would therefore be useful to find a way to do a dynamical study of collisions in near resonant optical lattices without the requirement of heavy computational resources.

We present here a simple method to calculate the rate of binary collisions in near-resonant optical lattices. The method is based on *single-atom* MCWF simulations<sup>20,21,22,23,24,25</sup> and the key idea is to monitor a quantum flux beyond the average distance  $z_a$  between the

atoms in a densely populated lattice. The accumulation of the atomic population beyond  $z_a$  gives information about the atomic quantum transport in a lattice and can be monitored by MCWF simulations for one atom. Thus, our method avoids the requirement of large computational resources of the two-atom MCWF collision simulations<sup>17,18,19</sup>.

To illustrate the usefulness of the method we calculate the collision rates for various modulation depths and occupation densities of one dimensional optical lattices. Moreover, we show that it is possible to obtain accurate collision rates for all the densities from only a few simulations for a given lattice. The simulation results show a quadratic behaviour of the binary collision rate as a function of density.

It has been shown before that, in the parameter regime we use here, the atomic motion between the lattice sites is to a good approximation dominated by the laser-atom interactions<sup>17,18</sup>. The effects of the interactions between atoms come into play as soon as the two atoms try to occupy the same lattice site and collide. Thus the combination of the method presented here to calculate the binary collision rate, and the semiclassical methods accounting the effects of intra-well collisions<sup>8,9,26</sup>, can simplify the study of the effects of collisions on the dynamics of the atomic cloud trapped in a near-resonant optical lattice.

We present the lattice structure and our calculation method of the collision rate in the next section, the results for various lattice depths and occupation densities in Section 3, and conclude with the discussion in Section 4.

## 2. Optical lattice and collision rate

### A. *Sisyphus cooling in optical lattice*

We consider here atoms having ground state angular momentum  $J_g = 1/2$  and excited state angular momentum  $J_e = 3/2$  corresponding to alkali metal elements when the hyperfine structure is neglected, and use the atomic mass  $M$  of <sup>133</sup>Cs. The resonance frequency between the states

Table 1. Used parameters. Rabi frequency  $\Omega$ , detuning  $\delta$ , lattice modulation depth  $U_0$ , and saturation parameter  $s_0$ .

$\Omega(\Gamma)$	$\delta(\Gamma)$	$U_0(E_r)$	$s_0$
1.0	-3.0	259	0.054
1.5	-3.0	580	0.122
1.9	-3.0	936	0.195

is  $\omega_0$  so that  $\hbar\omega_0 = E_e - E_g$ , where  $E_e$  and  $E_g$  are energies of the ground and the excited states in zero field. A single atom has two ground state sublevels  $|g_{\pm 1/2}\rangle$  and four excited state sublevels  $|e_{\pm 3/2}\rangle$  and  $|e_{\pm 1/2}\rangle$ , where the half-integer subscripts indicate the quantum number  $m$  of the angular momentum along the  $z$  direction.

The laser field consists of two counter-propagating beams with orthogonal linear polarizations and with frequency  $\omega_L$ . The total field has a polarization gradient in one dimension and reads (after suitable choices of phases of the beams and origin of the coordinate system)

$$\mathbf{E}(z, t) = \mathcal{E}_0(\mathbf{e}_x e^{ik_r z} - i\mathbf{e}_y e^{-ik_r z})e^{-i\omega_L t} + c.c., \quad (1)$$

where  $\mathcal{E}_0$  is the amplitude and  $k_r$  the wavenumber.

The intensity of the laser field and the strength of the atom-field coupling is described by the Rabi frequency  $\Omega = 2d\mathcal{E}_0/\hbar$ , where  $d$  is the atomic dipole moment of the strongest transition between the ground and excited states. The detuning of the laser field from the atomic resonance is given by  $\delta = \omega_L - \omega_0$ . As a unit for  $\Omega$  and  $\delta$  we use the atomic linewidth  $\Gamma$ , and express energy in the recoil unit  $E_r = (\hbar^2 k_r^2)/2M$ .

We keep the detuning fixed,  $\delta = -3\Gamma$ , and vary the Rabi frequency  $\Omega$ , which gives various values for the optical potential modulation depth

$$U_0 = -\frac{2}{3}\hbar\delta s_0, \quad (2)$$

where  $s_0$  is the saturation parameter given by

$$s_0 = \frac{\Omega^2/2}{\delta^2 + \Gamma^2/4}. \quad (3)$$

See Table 1 for used parameters.

The system Hamiltonian after the rotating wave approximation reads

$$H_s = \frac{p^2}{2M} - \hbar\delta P_e + V. \quad (4)$$

Here  $P_e$  is the projector operator  $P_e = \sum_{m=-3/2}^{3/2} |e_m\rangle \langle e_m|$ , and the interaction between an atom and the field is

$$V = -i\frac{\hbar\Omega}{\sqrt{2}} \sin(kz) \left\{ |e_{3/2}\rangle \langle g_{1/2}| + \frac{1}{\sqrt{3}} |e_{1/2}\rangle \langle g_{-1/2}| \right\} \\ + \frac{\hbar\Omega}{\sqrt{2}} \cos(kz) \left\{ |e_{-3/2}\rangle \langle g_{-1/2}| + \frac{1}{\sqrt{3}} |e_{-1/2}\rangle \langle g_{-1/2}| \right\} \\ + h.c. \quad (5)$$

The position and time dependent wave function of the system is

$$|\psi(z, t)\rangle = \sum_{j,m} \psi_{j,m}(z, t) |jm\rangle. \quad (6)$$

The periodic polarization gradient of the laser field and the subsequent periodicity of the couplings between the atomic states are reflected in the periodic light shifts (ac-Stark shifts) of the atomic sublevels creating the optical lattice structure. When the atomic motion occurs in a suitable velocity range, optical pumping of the atom between the ground state sublevels reduces the kinetic energy of the atom<sup>1,2,3,4,5,6,7</sup>, and the atom is cooled.

When the steady state is reached after a certain period of cooling, atoms are to a large extent localized into the optical potential wells. In this study we deal with near-resonant optical lattices where the laser field is detuned a few atomic linewidths to the red of the atomic transition. Thus, after localization atoms may still move around in the lattice due to the finite extent of the atomic wave packet and scattering of photons which transfers the population between the various ground state sublevels and corresponding optical potentials via the optical pumping mechanism.

Because the atoms are able to move between the lattice sites, they may try to occupy the same site and collide. The purpose of this paper is to find a simple way to calculate the binary collision rate without the need to perform complicated two-atom simulations. We use the occupation densities  $\rho_0$  of the lattice between 14.2% and 25.0% corresponding to cases with every seventh and fourth site occupied respectively. Other relevant parameters are presented in Table 1. From the simulation results, it is possible to calculate the collision rates for a wide range of occupation densities of the lattice, see Section 4.

## B. Calculation of collision rate

### 1. Monitoring the quantum flux

The key idea in our method is to monitor the quantum flux beyond the average distance  $z_a$  between the atoms in the one dimensional lattice. Since the distance between the nearest neighbour lattice sites is  $\lambda/4$ , then, e.g.,  $z_a = \lambda$  corresponds to the occupation density  $\rho_0 = 25\%$  of the lattice. Here  $\lambda$  is the wavelength of the lattice lasers. We call the area  $|z| > z_a$  the accumulation region (see Fig. 1) and denote the time dependent fraction of the wave packet in this region by

$$|\psi_a|^2(t) = \int_{|z| > z_a} \psi^*(z, t)\psi(z, t) dz. \quad (7)$$

The ensemble averaged Monte Carlo (MC) result of  $|\psi_a|^2(t)$  gives information about the number of collisions and the collision rate, as shown below.

To get the value for a collision rate we need to know how many atoms have travelled into the accumulation region and in which time. Thus, we need information

about the quantum flux *into* the accumulation region, in other words the *cumulative* population in the accumulation region as a function of time. This means that we should be able to make the quantum flux unidirectional into  $|z| > z_a$ . The atoms should therefore be able to arrive into the accumulation region due to their random motion in the lattice but should not be allowed to leave. In this case the accumulation rate of the atomic population into the accumulation region could give us the binary collision rate in the lattice.

To make the quantum flux unidirectional into the accumulation region we add the diagonal term

$$H_m = \begin{cases} 0 & : |z| < z_a - \lambda/8, \\ -\alpha & : |z| > z_a + \lambda/8, \\ -\alpha \cos^2 \left[ 2\pi \left( \frac{z+z_a}{\lambda} + 1/8 \right) \right] & : -z_a - \lambda/8 \leq z \leq -z_a + \lambda/8, \\ -\alpha \sin^2 \left[ 2\pi \left( \frac{z-z_a}{\lambda} + 1/8 \right) \right] & : z_a - \lambda/8 \leq z \leq z_a + \lambda/8 \end{cases} \quad (8)$$

to the system Hamiltonian, Eq.(4). We show the total optical potentials for the two ground state sublevels in Fig. 1. The steady state momentum distributions and the average kinetic energy of the atoms in the region  $|z| < z_a$  agree with the already known results for optical lattices, see for example Ref. 27.

When an atom arrives into a lattice site located around  $\pm z_a$ , corresponding to a collision site, it is pushed into the accumulation region and is not allowed to climb back to the region  $|z| < z_a$ . This does not change the physics for region  $|z| < z_a$  before the atom reaches collision site. After arrival the atom is captured into the accumulation region and as a consequence it is easy to calculate the cumulative population as a function of time. The trick here is that the drop in energy can not be too large but has to be large enough: Sisyphus cooling should still be effective in accumulation region, preventing the atoms from simply bouncing back from the wall of the grid and traveling back to  $|z| < z_a$ ; but the energy drop has to be large enough so that the probability to climb the energy barrier from the accumulation region should be small. We have chosen the values  $\alpha = 375, 840, 1356 E_r$  for  $U_0 = 259, 580, 936 E_r$  respectively.

The total Hamiltonian for the time evolution of the system now reads

$$H = H_s + H_m + H_d, \quad (9)$$

where  $H_s$  is the system Hamiltonian from Eq. (4),  $H_m$  the optical potential modification from Eq. (8), and  $H_d$  includes the non-Hermitian decay part of the MC method (see below).

## 2. Monte Carlo wave function method

We use the MCWF method (see Refs. 20-23. for details, and, e.g., Refs. 24-26 for applications of the method to the cold collision problems) to calculate the collision rates. We have also applied the method recently to study heating in red-detuned<sup>17,18</sup> and optical shielding in blue-detuned lattices<sup>19</sup>.

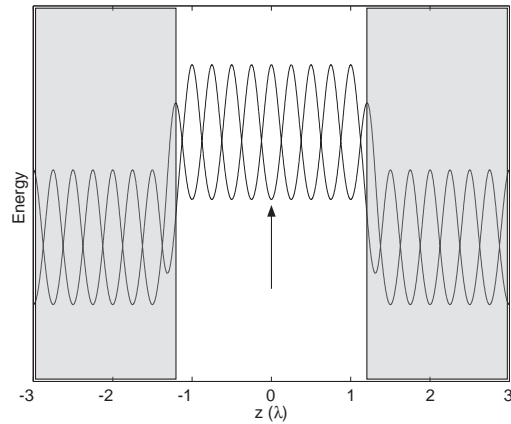


Fig. 1. The schematic view of the optical potentials for the two ground state Zeeman sublevels. The initial lattice site of the wave packet is indicated by the arrow and the modification of the potentials around the points  $\pm z_a$  makes the quantum flux unidirectional into the accumulation region (shown as shaded area).

The core idea of the MCWF method is to generate a large number of single wave function time evolution histories which include stochastic quantum jumps. The jumps occur because of the non-Hermitian part  $H_d$  in the system Hamiltonian. The information about the decay of the system is included in  $H_d$ , which shrinks the norm of the wave function and gives the jump probability for each time step taken<sup>28</sup>. The results for the system properties are finally obtained as an ensemble average of the generated single wave function histories.

The initial position of the wave packet in our simulations is given randomly into the lattice well around the point  $z = 0$  (see Fig. 1), and with zero mean momentum. Strictly speaking we should use as initial position and momentum distributions the steady state distributions for the used lattice parameters. We emphasize that the time scale to achieve the steady state is short compared to the population accumulation time to the accumulation region and we have checked that the change of the initial conditions does not change the simulation results. Thus, we avoid doing the double effort (first calculating the steady state properties of the system and then the collision rate) but still get the correct results. If one does simulations for higher occupation densities than used here (which is not actually necessary since the simulation results calculated here can be used to obtain the rate curve for wide range of densities, see Section 3), then more care should be given to the initial conditions of the system.

The number of the generated wave function histories per simulation varies from 256 to 320 and the total simulation times vary from  $3200\Gamma^{-1}$  to  $6400\Gamma^{-1}$ .

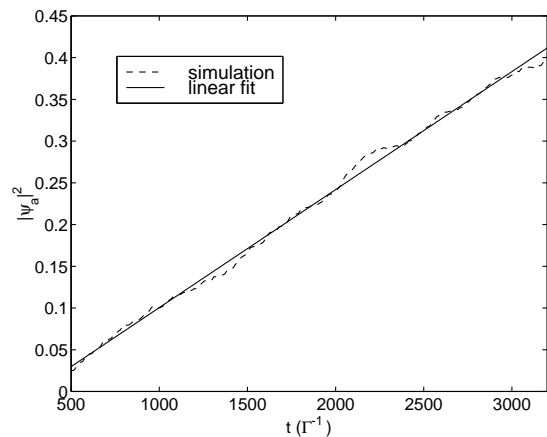


Fig. 2. An example ( $U_0 = 936E_r$ ,  $\rho_0 = 20\%$ ) of the accumulation region population  $|\psi_a|^2$  as a function of time. The binary collision rate  $R$  is obtained from the slope of the curve  $\beta$  and the average distance between the atoms  $z_a$  as  $R = \beta/z_a$ , see text.

### 3. Collision rate

We show an example of the ensemble averaged atomic population in the accumulation region,  $|\psi_a|^2$ , as a function of time in Fig. 2 where we display the simulation result and the linear fit.

Figure 2 demonstrates a steady flow of atomic population into the accumulation region. Thus, by fitting a linear function to the MC simulation result we can use the slope of the curve,  $\beta$ , to calculate the collision rate  $R$  in the lattice.

In the example of Fig. 2  $|\psi_a|^2(t = 3000\Gamma^{-1}) \approx 0.4$  with the number of histories of 320. This means that the number of collisions in time  $t = 3000\Gamma^{-1}$  in this specific case was 0.4 per  $z_a$  or  $0.4 \times 320 = 128$  for a lattice length of  $320z_a$ .

In general, the collision rate from simulations per unit time and per unit volume (per unit length in our one dimensional lattice) is given by

$$R = \beta/z_a. \quad (10)$$

The total number of collisions  $N_{tot}$  in the experiment would thus be  $N_{tot} = R \times t \times L$  where  $t$  is time and  $L$  the length of the one dimensional lattice.

## 3. Results

We have simulated the binary collision rate  $R$  for three different lattice depths  $U_0$  with fixed detuning  $\delta = -3\Gamma$  (see Table 1), and for lattice occupation densities  $\rho_0 = 14.3\%$ ,  $16.7\%$ ,  $20\%$ ,  $25\%$ , from every seventh to every fourth lattice site occupied respectively. The results are displayed in Fig. 3.

The simulation results show a quadratic behaviour of  $R$  with respect to atomic density<sup>29</sup>. Thus we can obtain the whole collision rate curve for all densities of the specific

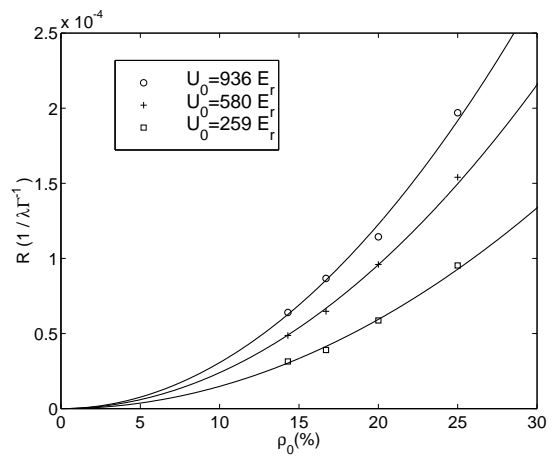


Fig. 3. The binary collision rate  $R$  for three different lattice depths  $U_0$  as a function of occupation density  $\rho_0$  of the lattice. The points show the simulation results and the solid lines the quadratic collision rate curves averaged from the simulation results for the specific lattice.

lattice by calculating  $R$  from only a single density MC result. By dividing the result for  $R$  with the square of the density it is possible to get the factor of quadratic behaviour for all densities. We note that this might be vulnerable to statistical error typical for MC simulations. To improve the statistical accuracy of the result for all densities we take the average of the quadratic factors obtained for the different densities. This makes it possible to obtain the whole collision rate curve for all the densities of the specific lattice with good statistical accuracy. The final results for all the density range obtained by averaging the various density MC results are drawn with solid lines in Fig. 3.

In the parameter regime we use, the motion between the lattice sites is mainly due to optical pumping, not because of the tunneling between the lattice sites. The higher is  $U_0$ , the larger is the collision rate. For fixed detuning the increasing field intensity means higher  $U_0$  and shorter optical pumping time. The atoms get more mobile since the increasing excited state population makes the probability of the internal state changing spontaneous emission event higher. If the atomic motion between lattice sites was because of tunneling, then the collision rate would decrease for tightly bound atoms for larger lattice modulation depths.

Moreover, the atomic motion between the lattice sites is not simply a random walk with a step size of the lattice constant. When the atom changes its internal state and optical potential well, it is not necessary that the atom halts its motion already in the nearest neighbour site. The atom may travel the distance of several lattice constants with a single flight, in fact, for the shallow optical lattices the atomic motion and diffusion in the lattice may even be anomalous and include Lévy walks<sup>30,31</sup>. For the parameters we use, the diffusion is normal<sup>32,33</sup>.

Since the atomic motion between the lattice sites here is due to optical pumping it is useful to compare the ratios of calculated collision rates of the various lattice depths to the corresponding ratios of the optical pumping times. The ratio of the optical pumping times for two different lattice depths with equal detuning is simply given by the square of the ratio of Rabi frequencies<sup>27</sup>. Here the ratio of the optical pumping times is on the same order of magnitude as the calculated ratios of the collision rates, but there can be a difference of factor of two. They do not match exactly because there is more to atomic motion between the sites than optical pumping only. For example the hopping statistics between the sites may differ for various lattice depths.

#### 4. Discussion and conclusions

We have presented a method to calculate the binary collision rate  $R$  in a steady state for an atomic cloud trapped in a near-resonant optical lattice. The method is based on MCWF simulations and the key idea is to monitor the quantum flux beyond the average distance between the atoms.

We have done the MCWF simulations for near-resonant lattice,  $\delta = -3\Gamma$ , and for lattice depths  $259E_r \leq U_0 \leq 936E_r$ . From the MCWF results it is possible to calculate the quadratic collision rate curve for all the densities of the lattice, within some limitations though (see below).

The advantage of the method is the avoiding of the large computational resource requirements of two-atom simulations. This is possible because in near-resonant lattices with large enough modulation depths the atomic motion between lattice sites is dictated by the field-atom interactions only<sup>17,18</sup>. The interactions between the atoms come into play only when two atoms try to occupy the same lattice site and collide (this is not the case for all parameter ranges, see Ref. 13). The method is also fast, straightforward, and fully quantum-mechanical.

In addition of giving quantitative estimate for the number of collisions in the experiment for a wide density range of optical lattices, our method brings out the possibility to combine two simple and computationally light methods to study collisions in optical lattices. Namely, the method presented here, combined with the semiclassical calculations accounting for the intra-well collision effects<sup>8,9,26</sup>, would simplify the study of the effects of the dynamic binary collisions for the atomic clouds trapped in optical lattices.

We have actually calculated here the collision rate for the primary collisions in the lattice. That is: the atomic cloud achieves the steady state and it is the steady state properties which define the collision rate here. Naturally the dynamics of the cloud may change when a large fraction of the atoms collide in short time for high occupation densities of the lattice. Moreover, the occupation density may change if the collided atoms gain enough kinetic energy to leave the lattice, or if the lattice is constructed

for metastable atoms<sup>10,11</sup>, which may ionize and escape the lattice when colliding. This is actually a benefit when using metastables, since it would be straightforward, at least in principle, to compare the number of collisions given by the method presented here and in the experiment.

We have to neglect the rescattering of photons. It is practically impossible account the rescattering effects because of finite amount of available computer resources. Despite of this, we think that our study is useful because of two reasons: a) we can give results for collision rates in the density region where the rescattering effects do not appear, b) because for very high densities (where rescattering effects should be accounted in principle) one could still use the method presented here to study the aspects of the binary collision effects on the lattice dynamics of the atomic cloud. This in itself is very complex problem, and also worth studying<sup>17,18,19</sup>.

From a Monte Carlo method point of view there is an interesting feature present here. Namely, we first do a few simulations and notice that the binary collision rate has a quadratic behaviour with respect to the atomic density. As a second step, we obtain the final results by taking the average of the various sets of MC results. We emphasize that this method differs from a simple increase of the number of histories in the MC ensemble to increase the statistical accuracy. Thus the benefits here are (in addition to the ones mentioned in previous paragraphs) twofold a) the statistical accuracy of the results increases b) the result can be obtained in a wider range than in which the MC simulations are done. This is a new feature in MCWF simulations to our knowledge, at least when MCWF method is applied to cold collision problems.

#### Acknowledgments

The author acknowledges financial support from the National Graduate School on Modern Optics and Photonics, discussions with Prof. K.-A. Suominen, the Finnish Center for Scientific Computing (CSC) for computing resources, and thanks Matt Mackie for critical reading of the manuscript.

#### References

1. J. Dalibard and C. Cohen-Tannoudji, "Laser cooling below the Doppler limit by polarization gradients: simple theoretical models", *J. Opt. Soc. Am. B* **6**, 2023-2045 (1989).
2. P. J. Ungar, D. S. Weiss, E. Riis, and S. Chu, "Optical molasses and multilevel atoms: theory", *J. Opt. Soc. Am. B* **6**, 2058-2071 (1989).
3. P. S. Jessen and I. H. Deutsch, "Optical lattices", *Adv. At. Mol. Opt. Phys.* **37**, 95-138 (1996).
4. D. R. Meacher, "Optical lattices - crystalline structures bound by light", *Contemp. Phys.* **39**, 329-350 (1998).
5. S. Rolston, "Optical lattices", *Phys. World* **11** (10), 27-32 (1998).

6. L. Guidoni and P. Verkerk, "Optical lattices: cold atoms ordered by light", *J. Opt. B* **1**, R23-R45 (1999).
7. H. J. Metcalf and P. van der Straten, *Laser Cooling and Trapping* (Springer, Berlin, 1999).
8. J. Weiner, V. S. Bagnato, S. Zilio, and P. S. Julienne, "Experiments and theory in cold and ultracold collisions", *Rev. Mod. Phys.* **71**, 1-85 (1999) and references therein.
9. K.-A. Suominen, "Theories for cold atomic collisions in light fields", *J. Phys. B* **29**, 5981-6007 (1996).
10. J. Lawall, C. Orzel, and S. L. Rolston, "Suppression and enhancement of collisions in optical lattices", *Phys. Rev. Lett.* **80**, 480-483 (1998).
11. H. Kunugita, T. Ido, and F. Shimizu, "Ionizing collisional rate of metastable rare-gas atoms in an optical lattice", *Phys. Rev. Lett.* **79**, 621-624 (1997).
12. E. V. Goldstein, P. Pax, and P. Meystre, "Dipole-dipole interaction in three-dimensional optical lattices", *Phys. Rev. A* **53**, 2604-2615 (1996).
13. C. Boisseau and J. Vigué, "Laser-dressed molecular interactions at long range", *Opt. Commun.* **127**, 251-256 (1996).
14. A. M. Guzmán and P. Meystre, "Dynamical effects of the dipole-dipole interaction in three-dimensional optical lattices", *Phys. Rev. A* **57**, 1139-1148 (1998).
15. C. Menotti and H. Ritsch, "Mean-field approach to dipole-dipole interaction in an optical lattice", *Phys. Rev. A* **60**, R2653-R2656 (1999).
16. C. Menotti and H. Ritsch, "Laser cooling of atoms in optical lattices including quantum statistics and dipole-dipole interactions", *Appl. Phys. B* **69**, 311-321 (1999).
17. J. Piilo, K.-A. Suominen, and K. Berg-Sørensen, "Cold collisions between atoms in optical lattices", *J. Phys. B* **34**, L231-L237 (2001).
18. J. Piilo, K.-A. Suominen, and K. Berg-Sørensen, "Atomic collision dynamics in optical lattices", *Phys. Rev. A* **65**, 033411 (2002) (16 pages).
19. J. Piilo and K.-A. Suominen, "Optical shielding of cold collisions in blue-detuned near-resonant optical lattices", *Phys. Rev. A* **66**, 013401 (2002) (9 pages).
20. J. Dalibard, Y. Castin, and K. Mølmer, "Wavefunction approach to dissipative processes in quantum optics", *Phys. Rev. Lett.* **68**, 580-583 (1992).
21. K. Mølmer, Y. Castin, and J. Dalibard, "Monte Carlo wavefunction method in quantum optics", *J. Opt. Soc. Am. B* **10**, 524-538 (1993).
22. K. Mølmer and Y. Castin, "Monte Carlo wavefunctions in quantum optics", *Quantum Semiclass. Opt.* **8**, 49-72 (1996).
23. M. B. Plenio and P. L. Knight, "The quantum-jump approach to dissipative dynamics in quantum optics", *Rev. Mod. Phys.* **70**, 101-144 (1998) and references therein.
24. M. J. Holland, K.-A. Suominen, and K. Burnett, "Quantal treatment of cold collisions in a laser field", *Phys. Rev. Lett.* **72**, 2367-2370 (1994).
25. M. J. Holland, K.-A. Suominen, and K. Burnett, "Cold collisions in a laser field: Quantum Monte Carlo treatment of radiative heating", *Phys. Rev. A* **50**, 1513-1530 (1994).
26. K.-A. Suominen, Y. B. Band, I. Tuvi, K. Burnett, and P. S. Julienne, "Quantum and semiclassical calculations of cold atom collisions in light fields", *Phys. Rev. A* **57**, 3724-3738 (1998).
27. Y. Castin, J. Dalibard, and C. Cohen-Tannoudji, "The limits of Sisyphus cooling", in *Proceedings of Light Induced Kinetic Effects on Atoms, Ion and Molecules*, L. Moi *et al.*, ed. (ETS Editrice, Pisa, 1991), pp. 1-24.
28. See Ref. 18 for the details of the jump operators that are used in our implementation of the method.
29. This is in agreement with the result given in Ref. 10 where the collisions are also a measure of atomic transport in a lattice and are independent of the scattering cross section.
30. F. Bardou, J. P. Bouchaud, O. Emile, A. Aspect, and C. Cohen-Tannoudji, "Subrecoil laser cooling and Lévy flights", *Phys. Rev. Lett.* **72**, 203-206 (1994).
31. S. Marksteiner, K. Ellinger, and P. Zoller, "Anomalous diffusion and Lévy walks in optical lattices", *Phys. Rev. A* **53**, 3409-3430 (1996).
32. W. Greenwood, P. Pax, and P. Meystre, "Atomic transport on one-dimensional optical lattices" *Phys. Rev. A* **56**, 2109-2122 (1997).
33. P. M. Visser and G. Nienhuis, "Quantum transport of atoms in an optical lattice" *Phys. Rev. A* **56**, 3950-3960 (1997).